# Detection and Characterization of Complexes of Methylmercury(II) with Duplex Deoxyribonucleic Acid and Synthetic Copolymers by Optical Detection of Magnetic Resonance†

Richard R. Anderson, August H. Maki,* and Christopher M. Ott

ABSTRACT: Complexes formed between $CH_3HgOH$ and the polynucleotide duplexes poly(dA)·poly(dT) and poly(dG)·poly(dC) and calf thymus DNA have been detected and characterized by luminescence and optically detected magnetic resonance (ODMR) spectroscopy. $CH_3HgOH$ is added by equilibrium dialysis at concentrations well below those previously found to cause denaturation of the duplex. Complexing of $CH_3Hg^{II}$ with the polynucleotide leads to heavy atom effects which are detected by the appearance of short-lived components in the phosphorescence decay. Heavy atom perturbed bases are identified by slow-passage ODMR frequencies and the lifetimes of phosphorescence transients induced by microwave rapid passage. Comparison of the zero-field splitting (zfs) parameters and signal polarity patterns with those found previously in specific mononucleotide and mononucleoside complexes with $CH_3Hg^{II}$ leads to the positive identification of complexed bases as well as the $CH_3Hg^{II}$ binding sites. We find that $CH_3HgOH$ at $10^{-5}$ M complexes with $N_3$ of thymine in poly(dA)·poly(dT) and with $N_7$ of guanine in both poly(dG)·poly(dC) at pH 6, and calf thymus DNA at pH 6.8. When $CH_3HgOH$ is added at $10^{-6}$ M, we find that complexing with poly(dA)·poly(dT) takes place, although binding does not occur at $N_3$ of thymine. The thymine triplet state properties are altered, but not necessarily as the result of a heavy-atom effect. Evidence for the presence of this type of complex in DNA treated with $10^{-5}$ M $CH_3HgOH$ is provided by the presence of thymine triplet states with properties similar to those observed in poly(dA)·poly(dT) treated at $10^{-6}$ M.

The complexing of mercurials with polynucleotides has been studied by a number of experimental methods (Yamane & Davidson, 1961; Millar, 1968; Clegg & Gruenwedel, 1979; Gruenwedel & Davidson, 1967; Gruenwedel & Lu, 1970; Chrisman et al., 1977; Walter & Luck, 1977). These studies all confirm that the primary binding sites of mercurials are the heterocyclic bases, rather than the nucleotide phosphates, which is expected from the mononucleotide binding studies of Simpson (1964). While methylmercury is observed to bind rather independently to the different base binding sites of denatured DNA, binding is reported to occur cooperatively with native DNA (Gruenwedel & Davidson, 1967; Gruenwedel & Lu, 1970) and with poly(dA-dT) (Gruenwedel, 1972) with simultaneous denaturation of the duplex. Chrisman et al. (1977), using differential Raman spectroscopy, have observed that complexing of $CH_3Hg^{II}$ with duplex calf thymus DNA takes place with no appearance of new bands when it is titrated with $CH_3Hg^{II}$ up to $r = 0.15$. ($r$ = DNA-bound $CH_3Hg^{II}$/nucleotide phosphate.) At $r = 0.30$, extensive binding to $N_3$ of thymidine (dThd) and $N_1$ of deoxyguanosine (dGuo) is observed in Raman spectra. These results suggest that complexing of $CH_3Hg^{II}$ takes place with DNA in the absence of denaturation. If this is indeed the case, the earlier experimental methods have not been capable of either detecting these complexes or giving direct information about the nature of the binding sites.

We report here the results of spectroscopic measurements of the reaction of $CH_3HgOH$ at extremely low concentrations with the synthetic duplex homopolymers poly(dA)·poly(dT) and poly(dG)·poly(dC), as well as with calf thymus DNA. The concentration of methylmercury in our measurements is kept well over an order of magnitude below that found to be required for denaturation of poly(dA-dT) (Gruenwedel, 1972), in order that complexes of $CH_3Hg^{II}$ with duplex DNA, if they occur, can be selectively observed. We take advantage of the heavy-atom effect (Kasha, 1952) which is expected to be induced when $CH_3Hg^{II}$ forms a complex directly with a heterocyclic base. The heavy-atom effect is an extremely close-range interaction requiring the approach of the Hg atom to within the sum of the van der Waals radii of the affected base. The heavy atom effect enhances intersystem crossing rates, leading to an enhancement of the triplet yield of a complexed base. In addition, the phosphorescence lifetime is drastically reduced, frequently the result of preferential enhancement of the radiative rate constants (Giachino & Kearns, 1970a,b). Thus, a heavy-atom effect can be readily detected by a reduction in the phosphorescence lifetime or the appearance of short components in the normal phosphorescence of a biopolymer.

Identification of the complexed base is made possible by measurement of a distinguishable property of the excited triplet state, the zero-field splitting (zfs)[1] parameters, $D$ and $E$. Although the zfs allows us to identify the unperturbed nucleotide triplet states (Eisinger & Shulman, 1968; Hoover et al., 1974), perturbations are expected from $CH_3Hg^{II}$ complexing, resulting in shifts of $D$ and $E$. We have previously measured the zfs of the various complexes formed between $CH_3Hg^{II}$ and the common mononucleotides occurring in DNA (Anderson & Maki, 1977) and have found that in the case of the purines in particular, the zfs parameters change significantly in the complex and they vary with the binding site. We find the triplet-state lifetimes of the complexed nucleotides to be on the order of 20 ms. We use the method of optical detection of magnetic resonance (ODMR) in zero applied field (El-Sayed, 1972; Kwiram, 1972) which discriminates in favor of the *more radiative* triplet states. The measurements also are made in a time-resolved manner to further discriminate

† From the Department of Chemistry, University of California, Davis, California 95616. *Received March 5, 1980.* This work was partially supported by a research grant (ES-01268) from the National Institute of Environmental Health Sciences and the Environmental Protection Agency.

[1] Abbreviations used: zfs, zero-field splitting; ODMR, optical detection of magnetic resonance; pM, –log [M], where [M] is the total molarity of all uncomplexed $CH_3Hg^{II}$ species; dTMP, deoxythymidine 5′-phosphate; EEDOR, electron–electron double resonance.

0006-2960/80/0419-4412$01.00/0 

in favor of *short-lived* triplet states. The triplet sublevel lifetimes of each transition are observed as microwave transients following a microwave pulse or fast passage through the signal region (Winscom & Maki, 1971) in order to ensure that ODMR signals originate from heavy atom perturbed triplet states with short lifetimes.

## Materials and Methods

Poly(dA)·poly(dT) (P-L Biochemicals) and calf thymus DNA (Worthington) were dissolved in 5 mM cacodylate buffer, pH 6.8, containing 50 mM $Na_2SO_4$ and 0.5% glucose. Poly(dG)·poly(dC) (Boehringer Mannheim) was dissolved in 5 mM phosphate buffer, pH 7.4, containing 50 mM $Na_2SO_4$ and 0.5% glucose. Polynucleotide concentration was made 1 mM in nucleoside phosphate by optical absorption measurement on a Cary 17 spectrophotometer. Methylmercury was added to poly(dA)·poly(dT) and DNA by equilibrium dialysis for several days with the same buffer containing $CH_3HgOH$ at either pM 6 or pM 5 with daily changes of buffer. The dialysis tubing ($^1/_4$ in.; A. H. Thomas Co.) was prepared conventionally and then stored before use in buffer containing $CH_3HgOH$ at either pM 6 or pM 5 with frequent changes of buffer. Poly(dG)·poly(dC) was dialyzed for several days against a 5 mM pH 6.0 phosphate buffer containing 50 mM $Na_2SO_4$, 0.5% glucose, and $CH_3HgOH$ at pM 5, with daily changes of buffer. Methylmercury(II) hydroxide was purchased with Alfa Inorganics, Inc., and was used to prepare a stock solution which was standardized by reported procedures (Waugh et al., 1955).

Methylmercury compounds are extremely toxic and adequate precautions were taken to ensure its safe containment. Although $CH_3HgOH$ and its salts generally are nonvolatile, volatile dimethylmercury may form under some circumstances, such as storage in concentrated solution. All storage or handling of methylmercury compounds was carried out in a dedicated, well ventilated fume hood. Gloves, gown, and face mask were worn when working with methylmercury. All wastes were stored in either a solid or a liquid waste jar within the hood; these were sealed and removed on occasion for safe disposal. In practice, methylmercury only left the hood in significant amounts as samples (which were returned after measurment for disposal) or when contained in the sealed storage jars.

Phosphorescence decay measurements were made at several reduced temperatures; the decay curves were signal averaged and deconvoluted by computer using a previously described curve-peeling procedure (Maki & Co, 1976). The sample generally was excited at 290 nm by using ~10-nm band-pass. Excitation of poly(dG)·poly(dC) was at 275 (uncomplexed) and 295 nm (complexed). The excitation source was a 100-W high-pressure mercury arc equipped with an aqueous infrared filter. For all measurements, the sample was contained in a 1 mm i.d. suprasil quartz tube and was frozen rapidly by direct immersion into the refrigerant. Slow-passage ODMR measurements were made by using the apparatus and methods described previously (Maki & Co, 1976). For these measurements the sample temperature was maintained at 1.1–1.2 K by pumping on the liquid helium refrigerant. Slow-passage measurements were made by sweeping the microwaves in both directions at the same rate and averaging the observed peak frequencies, to compensate for fast-passage effects. The sweep repetition rate was chosen to be fast enough to discriminate against signals from long-lived triplet states while still giving reasonably undistorted signals from the short-lived $CH_3Hg^{II}$-perturbed triplet states. This time-resolution method has been described previously (Anderson & Maki, 1977) in connection with ODMR measurements of $CH_3Hg^{II}$ complexes of the mononucleosides and mononucleotides. Microwave-induced phosphorescence transients were obtained and analyzed by previously described methods (Winscom & Maki, 1971). Optically detected electron–electron double resonance (EEDOR) was done on the poly(dG)·poly(dC) complexes in order to improve the signal intensities. This method has been described previously (Kuan et al., 1970); we modified this procedure somewhat in order to compensate for the broad, inhomogeneous ODMR lines typically found in biopolymers. The pumping microwaves were frequency modulated through the inhomogeneous ODMR signal width instead of being applied at a sharp frequency.

Table I: Phosphorescence Decay Data of Polynucleotides and Their $CH_3Hg^{II}$ Complexes[a]

| | phosphorescence intensity (%) | | | | | |
|---|---|---|---|---|---|---|
| | $T = 77$ K | | | $T = 4.2$ K | | |
| | pM ∞ | pM 6 | pM 5 | pM ∞ | pM 6 | pM 5 |
| poly(dA)·poly(dT)[b] | | 0 | 96 | 0 | 0[c] | 93 |
| poly(dG)·poly(dC) | 0[d] | | 14[e] | 0[d] | | 54[e] |
| calf thymus DNA[b] | 0 | | 50 | 0 | | 26 |

[a] Entries are the percent of the steady-state phosphorescence intensity which decays with $1/e$ lifetimes of 50 ms or less. Decay was measured with 2-nm slit width. [b] $\lambda_{obsd} = 440$ nm. [c] At 1.1 K, 20% of the phosphorescence intensity decays with a lifetime of ~30 ms. This short component at 1.1 K is not observed at pM ∞. [d] $\lambda_{obsd} = 420$ nm. [e] $\lambda_{obsd} = 465$ nm.

## Results

The phosphorescence decay kinetics of all samples were found to be nonexponential at both 77 and 4.2 K. Deconvolution of the phosphorescence decay of the uncomplexed polynucleotides in a multiexponential expansion revealed no lifetime components present which were shorter than 100 ms. Shorter lifetime components were observed in the phosphorescence deconvolution of each polynucleotide which had been treated with $CH_3Hg^{II}$ at pM 5, as well as in poly(dA)·poly(dT) at 1.1 K treated at pM 6. In Table I, we list the fraction of steady-state phosphorescence intensity decaying with lifetimes below 50 ms. This decay constant was chosen arbitrarily as an upper limit for $CH_3Hg^{II}$-perturbed triplet lifetimes, since all the $CH_3Hg^{II}$–monomer complexes were found to have phosphorescence lifetimes below this value (Anderson & Maki, 1977). These data indicate that $CH_3Hg^{II}$ complexing with the bases of each of the polynucleotides occurs at pM 5 and possibly with poly(dA)·poly(dT) at pM 6.

In Table II, we list the ODMR signals observed in the uncomplexed and complexed polynucleotides, as well as those observed previously for the mononucleotides and mononucleosides complexed with $CH_3Hg^{II}$ at specific sites.

The sublevel lifetimes observed in the decay of the phosphorescence transient produced by microwave rapid passage through the zero-field transitions (Winscom & Maki, 1971) are given in Table III for the synthetic polynucleotide duplexes.

## Discussion

*(A) Poly(dA)·Poly(dT) at pM 6 and 5.* Slow-passage signals are observed in poly(dA)·poly(dT) at pM ∞ and are assigned to T based on the agreement of the zfs parameters with those of dTMP (Eisinger & Shulman, 1968). No ODMR signals from the A triplet state are observed. It should be noted that the T ($N_3$)–methylmercury complex of dTMP has effectively the same $D$ and $E$ parameters as uncomplexed dTMP (Table I). The slow-passage ODMR spectra of the $\nu_2$–$\nu_3$ region of poly(dA)·poly(dT) at pM ∞, 6, and 5 are compared

Table II: Triplet-State Data for $CH_3Hg^{II}$-Nucleic Acid Complexes[a]

| nucleic acid (binding site) | pM | $\nu_1$[b] (GHz) | $\nu_2$[b] (GHz) | $\nu_3$[b] (GHz) | $D/(hc)$[c] ($cm^{-1}$) | $E/(hc)$[c] ($cm^{-1}$) | assignment |
|---|---|---|---|---|---|---|---|
| dTMP ($N_3$) | | 0.77 [+] (260) | 5.53 [+] (430) | 6.26 [+] (380) | 0.197 | 0.0128 | |
| CMP ($N_3$) | | 1.03 [+] (230) | 5.40 [+] (595) | 6.48 [+] (385) | 0.198 | 0.0172 | |
| 3-MeCyd ($NH_2$) | | 0.79 [+] (135) | 5.52 [+] (280) | 6.32 [+] (358) | 0.197 | 0.0132 | |
| AMP ($N_1$) | | 1.78 [+] (168) | 2.28 [−] (158) | 4.06 [+] (198) | 0.106 | 0.0297 | |
| 1-MeAMP ($NH_2$ or $N_7$) | | 1.57 [+] (164) | 2.50 [+] (237) | 4.12 [+] (363) | 0.110 | 0.0262 | |
| GMP ($N_7$) | | 1.22 [+] (250) | 4.54 [−] (830) | 5.80 [−] (778) | 0.172 | 0.0203 | |
| 1-MeGuo ($N_7$) | | 1.27 [+] (215) | 4.48 [−] (943) | 5.70 [−] (838) | 0.170 | 0.0212 | |
| GMP ($N_1$) | | 1.08 [+] (110) | 3.63 [+] (220) | *d* | 0.139 | 0.0180 | |
| poly(dA)·poly(dT) | ∞ | 0.69 [+] (279) | 5.57 [−] (237) | 6.37 [−] (347) | 0.198 | 0.0120 | T |
| | 6 | 0.63 [+] (504) | 5.56 [−] (499) | 6.29 [+] (390) | 0.198 | 0.0113 | T |
| | 5 | 0.81 [+] (194) | 5.60 [+] (268) | 6.45 [+] (368) | 0.201 | 0.0138 | T ($N_3$) |
| poly(dG)·poly(dC) | ∞ | 1.09 [+] (270) | 3.61 [+] (460) | 4.67 [+] (250)[e] | 0.138 | 0.0179 | G |
| | 5 | 1.19 [+] (213) | 4.95 [−] (380)[f] | 6.34 [−] (820)[f] | 0.188 | 0.0215 | G ($N_7$) |
| DNA calf thymus | ∞[g] | 0.75 (200) | 5.72 (400) | 6.46 (300) | 0.203 | 0.0123 | T |
| | 5 | 0.69 [+] (315) | 5.46 [−] (370)[h] | 6.22 [+] (380) | 0.195 | 0.0121 | T |
| | | 1.37 [−] (420) | 4.58 [−] (900) | 5.99 [−] (670)[h] | 0.176 | 0.0232 | G ($N_7$) |

[a] Mononucleotide and -nucleoside data are from Anderson & Maki (1977). Data for poly(dA)·poly(dT) are from Anderson (1979). [b] [+] and [−] refer to an increase or decrease in phosphorescence intensity, respectively, for the slow-passage signals. Line width (full width at half-maximum) in MHz is in parentheses. The uncertainty in $\nu_i$ is approximately ±0.1 × width. [c] zfs is given by using the arbitrary assignment $\nu_1 = 2|E|/h$. Signs of $D$ and $E$ are not known. [d] Signal is obscured by $\nu_2$ signal of G ($N_7$) complex which is present in sample. [e] Signal is only observed by using EEDOR, where the $\nu_1$ transition is pumped. [f] Signals appear to be structured; see Figure 4. [g] Data are from Dinse & Maki (1976). Signals are not observed during continuous optical pumping. [h] These frequencies have greater error due to considerable spectral overlap.

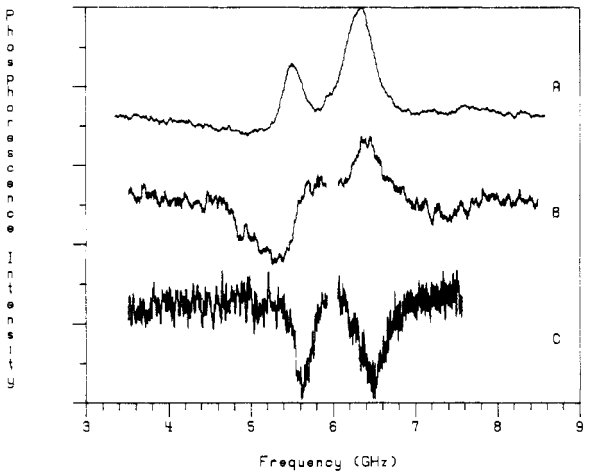


FIGURE 1: Slow-passage $\nu_2$ and $\nu_3$ signals of (C) poly(dA)·poly(dT) and its complex with $CH_3Hg^{II}$ (A) at pM 5 and (B) at pM 6. $T$ = 1.1–1.2 K. (A) Frequency is swept from 8.3 to 3.7 GHz at 4.0 GHz/s. The signal is the result of 750 accumulations. (B) Signals result from separate measurements; microwaves are swept from 6.0 to 3.7 GHz and from 6.0 to 7.5 GHz at 2.0 GHz/s. Each signal results from 3000 accumulations. (C) Signals result from separate measurements; sweep ranges are the same as in (B), but the sweep rate is 220 MHz/s. The low-frequency signal results from 1024 accumulations, and the high frequency signal results from 2500 accumulations.

in Figure 1. As pM decreases in this range, the polarity of the signals change from [−][−] to [−][+] to [+][+]. The intermediate nature of the pM 6 spectrum indicates that effects of $CH_3Hg^{II}$ complexing with the polymer are already evident in the ODMR at this equilibrium concentration of free $CH_3HgOH$. In Figure 2, we compare the phosphorescence transients induced by microwave rapid passage through the $\nu_2$ transition of poly(dA)·poly(dT) at pM ∞ and 5. The rapid decay of the transient at pM 5 in comparison with pM ∞ indicates that the lifetimes of the triplet sublevels connected by the $\nu_2$ transition are reduced as a result of a heavy-atom perturbation. We have made similar transient measurements on the other ODMR transitions of poly(dA)·poly(dT) with the results given in Table III. In poly(dA)·poly(dT), a reduction in the transient lifetimes of each ODMR transition is observed as [$CH_3HgOH$] increases. The effect of initial stages of

Table III: Decay Lifetimes of Phosphorescence Transients Induced by Microwave Rapid Passage[a]

| | pM | $\tau_1$ (ms) | $\tau_2$ (ms) | $\tau_3$ (ms) |
|---|---|---|---|---|
| poly(dA)· poly(dT) | ∞ | 110 | (390) | 110 [1.9] (520) [1.0] |
| | 6 | 100 | (250) | 90 |
| | 5 | 10 | 10 [18] (140) [1] | 12 [17] (160) [1] |
| poly(dG)· poly(dC) | ∞ | 360 | 260 | |
| | 5 | (4) | (7) | <2[b] [>2.8] (22) [1] |

[a] The transient response decay lifetime(s) of the $\nu_i$ transition is (are) indicated by $\tau_i$. Negative (phosphorescence intensity decrease) initial transients are in parentheses. Each response is fit to a maximum of two exponential decay components by using a least-squares routine. When both a positive transient and a negative transient are observed, the relative preexponential factors are given in brackets. [b] The transient decay is more rapid than the passage time through the resonance.

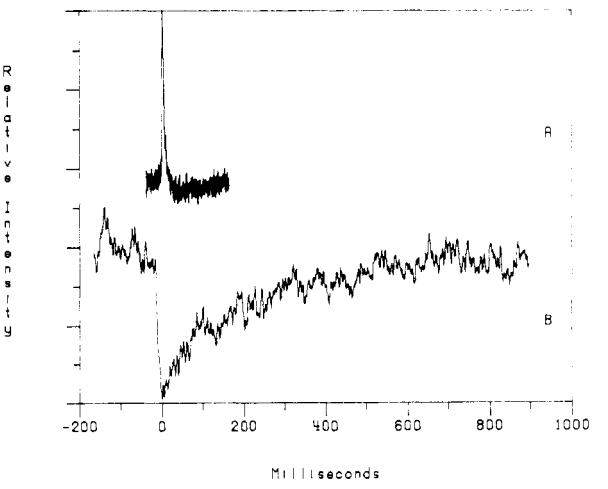


FIGURE 2: Microwave-induced phosphorescence transient resulting from rapid passage through the $\nu_2$ signal of poly(dA)·poly(dT). Rapid passage occurs at $t$ = 0. (A) pM 5, 3000 accumulations; (B) uncomplexed, 4096 accumulations. $T$ = 1.1–1.2 K.

$CH_3Hg^{II}$ complexing is most apparent in the transient response at $\nu_3$ where a rather prominent long-lifetime negative transient

which is seen at pM ∞ is no longer observable at pM 6. The disappearance of this negative component of the transient response is consistent with the change of the polarity of the slow-passage $\nu_3$ signal from [−] to [+] as pM goes from ∞ to 6. At pM 5, where further complexing with $CH_3Hg^{II}$ has occurred, each signal contains a prominent component of ~10 ms in its transient response. This order of magnitude for the sublevel lifetimes is expected for a complex having $CH_3Hg^{II}$ bound directly to T and agrees with that found for the dTMP ($N_3$) complex. There is also close agreement of the zero-field ODMR frequencies (Table II). According to the equilibrium constant measurements of Gruenwedel & Davidson (1966) and Chrisman et al. (1977), on complex formation between dThd and $CH_3HgOH$, ~20% of dThd $N_3$ sites should be complexed with $CH_3Hg^{II}$ at pM 5 in a sample of the mononucleoside or in single-stranded poly(dT). The presence of $CH_3HgOH$ at pM 5 is not expected to cause denaturation of the poly(dA)·poly(dT) on the basis of sedimentation rate measurements on the alternating copolymer poly(dA-dT) where strand separation was not observed until pM 4 (Gruenwedel, 1972). We find that poly(dA)·poly(dT) melts sharply at 65 °C, at both pM 5 and ∞. The hyperchromism accompanying melting is 14% less at pM 5, however. The ODMR measurements do not permit the quantitative determination of the number of complexed bases. Unusually intense signals may occur from relatively few complexed bases in a stacked polymer due to the possibility of sensitization of the complexes by energy transfer from excited uncomplexed bases. Qualitatively, the ODMR signals have a signal/noise comparable to that observed in samples of the $CH_3Hg^{II}$–dTMP ($N_3$) complex at the same concentration of nucleoside phosphate [compare Figure 1A with Figure 1 of Anderson & Maki (1977)]. We believe, therefore, that complexing at pM 5 is not restricted to the single-stranded regions of oligo(dT) which may be present to some extent in poly(dA)·poly(dT). It appears, then, that complexing of $CH_3Hg^{II}$ with double-stranded regions of poly(dA)·poly(dT) occurs, leading to heavy-atom effects on the thymine bases. There is a significant upward shift (190 MHz) of the $\nu_3$ signal of the poly(dA)·poly(dT) complex relative to the $N_3$ complex of dTMP which suggests that there are local structural differences in the complex in these systems. We suggest that complexing of $CH_3Hg^{II}$ takes place at $N_3$ of thymine with the displacement of a proton, with local disruption of the duplex structure, but without strand separation.

The ODMR signals observed from poly(dA)·poly(dT) complexed with $CH_3Hg^{II}$ at pM 6 are not from the same species as those observed at pM 5 or from $CH_3Hg^{II}$–dTMP ($N_3$). The effect of adding $CH_3Hg^{II}$ at pM 6 to poly(dA)·poly(dT) is quite subtle as far as the thymine signals are concerned. The microwave-induced transient lifetimes observed in Table III hardly differ from those observed in uncomplexed poly(dA)·poly(dT). The slow-passage $\nu_3$ signal becomes [+], which is a consequence of the disappearance of a prominent slow negative component of the transient phosphorescence response to rapid passage through $\nu_3$. These observations are not consistent with the presence of a mixture of signals from $N_3$ complexes and uncomplexed bases but rather with the presence of a different type of complex at pM 6.

*(B) Poly(dG)·Poly(dC) at pM 5.* When $CH_3Hg^{II}$ is complexed with poly(dG)·poly(dC) at pM 5, extremely fast responses are observed in the transient measurements relative to the uncomplexed polymer. These data are given in Table III. The heavy atom perturbed triplet lifetimes are considerably shorter in poly(dG)·poly(dC) than they are in poly(dA)·poly(dT). The transient response to microwave fast passage through the $\nu_3$ transition of poly(dG)·poly(dC) (pM 5) is compared with the response to the same fast-passage signal in the $CH_3Hg^{II}$ complex of 1-MeGuo ($N_7$ complex) in Figure 3. The similarity of these responses indicates that the radiative and radiationless decay constants of the sublevels connected by $\nu_3$ follow a similar pattern in the two complexes, although both decay lifetimes are shorter in poly(dG)·poly(dC). In particular, the weakness of the positive, short-lived component of the response indicates that the short-lived sublevel of this transition has a relatively low radiative quantum yield, which is the reason why the slow-passage $\nu_3$ signal of both the poly(dG)·poly(dC) complex and the $N_7$ complexed monomer Guo models is negative (Table II).

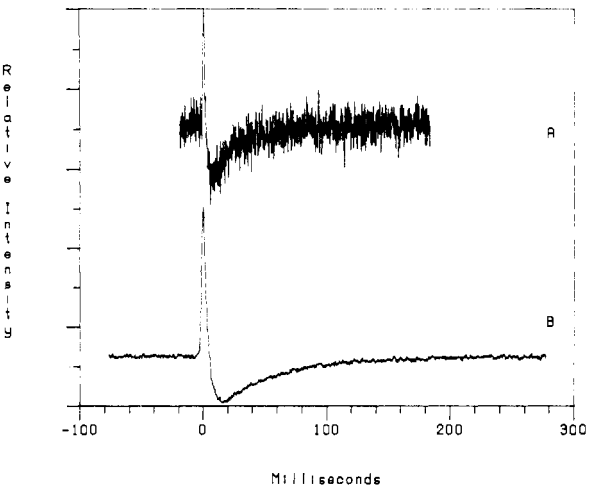


FIGURE 3: Microwave-induced phosphorescence transients induced by rapid passage (at $t = 0$) through the G $\nu_3$ signal. (A) Poly(dG)·poly(dC) at pM 5, 65000 accumulations; (B) 1-MeGuo ($N_7$)–$CH_3Hg^{II}$ complex at $c$ = 1 mM, 6000 accumulations. $T$ = 1.1–1.2 K.

The slow-passage ODMR signals observed in poly(dG)·poly(dC) at pM ∞ are extremely weak, and we were not able to observe the $\nu_3$ signal without the use of EEDOR. The zfs frequencies are the same as those assigned to G in ApG (Hoover et al., 1974) within experimental error. The low intensity of the signals in the homopolymer suggests that they may be due to unstacked bases in single-stranded regions. This is supported by the close agreement of the zfs with ApG in which G is not base paired or stacked. We expect that stacking of aromatic molecules will lead to measurable changes in the triplet-state zfs (Co & Maki, 1978).

Complexing of poly(dG)·poly(dC) with $CH_3Hg^{II}$ at pM 5 (pH 6) leads to the appearance of new signals at very different frequencies from short-lived triplet states, two of which are shown in Figure 4. An additional [+] transition which appears at 1.19 GHz is not shown. For comparison, the $\nu_2$ and $\nu_3$ signals of GMP ($N_7$ $CH_3Hg^{II}$ complex) as well as the effect of EEDOR (microwave pumping of the $\nu_1$ transition) on the poly(dG)·poly(dC) spectrum are presented. The effect of EEDOR on the general appearance of this transition region is evidence for a great degree of heterogeneity in the local environments of the $CH_3Hg^{II}$ complexes. We will return to this point below. The signals from poly(dG)·poly(dC) are seen to resemble those of $CH_3Hg^{II}$–GMP ($N_7$) in the $\nu_2$, $\nu_3$ region. As can be seen from Table II, the ODMR frequencies are far removed from those obtained from the $N_1$ complex of GMP. At pM 5, pH 6, about 1% of the $N_7$ sites of dGuo should be complexed with $CH_3Hg^{II}$ (Simpson, 1964) in a sample of noninteracting monomers. The intensity of the signals observed from poly(dG)·poly(dC) relative to those from $CH_3Hg^{II}$–GMP

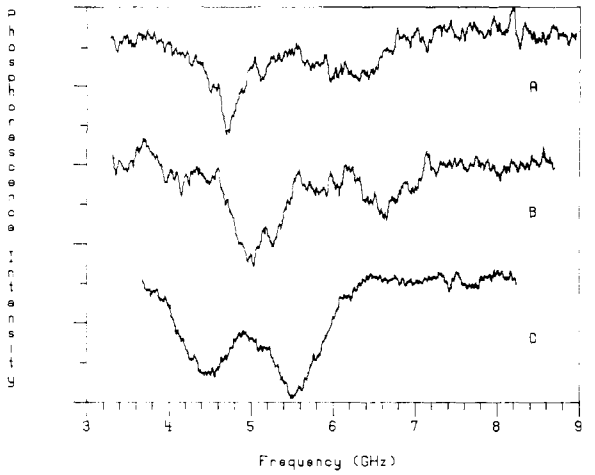


FIGURE 4: ODMR slow-passage signals in the $\nu_2$–$\nu_3$ signal region of dGuo ($N_7$)–$CH_3Hg^{II}$. (A) Poly(dG)·poly(dC) at pM 5, pH 6. Microwaves are swept from 3.7 to 8.3 GHz at 1.53 GHz/s. Signals result from 4000 accumulations. (B) Same sample showing the effects of EEDOR on the signals. Microwaves are swept from 3.7 to 8.3 GHz at 9.2 GHz/s. The dGuo ($N_7$)–$CH_3Hg^{II}$ $\nu_1$ signal is continuously excited during the measurement. The signals result from 30 000 accumulations. (C) $CH_3Hg^{II}$–GMP ($N_7$), $c$ = 1 mM. Microwaves are swept from 8.0 to 3.7 GHz at 4.3 GHz/s. The signals result from 348 accumulations. $T$ = 1.1–1.2 K.

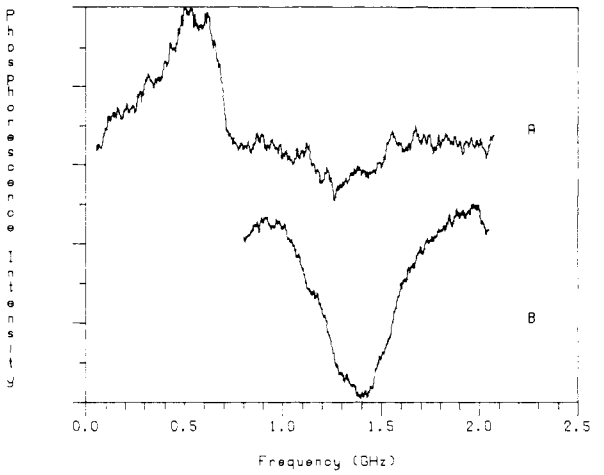


FIGURE 5: Slow-passage ODMR signals in the $\nu_1$ signals region of calf thymus DNA complexed with $CH_3Hg^{II}$ at pM 5. (A) Microwave frequency is swept from 2.0 to 0.2 GHz at 1.6 GHz/s. The signal results from 2098 accumulations. (B) Microwave frequency is swept from 0.9 to 2.0 GHz at 10 GHz/s. The signal results from 20 600 accumulations. $T$ = 1.1–1.2 K.

($N_7$) are in rough accord with this prediction. We can estimate that the signal intensities of the polymer sample are consistent with complexing of roughly 1% of the dGuo ($N_7$) sites in the sample, so we have no evidence for enhanced binding affinity at this site in the polynucleotide. The polymer signals in the 4–7-GHz range are shifted significantly in frequency relative to the two resolved signals of the monomer complex, and they are structured, indicating that the G complexes of poly(dG)·poly(dC) do not occur in a homogeneous local environment. This interpretation is supported further by the effect of EEDOR enhancement of the signal region (Figure 4B). The major peaks shift to higher frequencies in the EEDOR spectrum, indicating that there is a considerable distribution of zfs parameters in the sample. The differences between the major peak frequencies of the EEDOR-enhanced spectrum of the polynucleotide and the $\nu_2$ and $\nu_3$ frequencies of $CH_3Hg^{II}$–GMP ($N_7$) arise from differences in local environment. A possible explanation of these differences is the presence of stacked as well as base-paired dGuo in the polynucleotide. The structure in this region may result from complexes in both duplex and single-stranded regions. No heavy atom perturbed signals are observed from poly(dG)·poly(dC) at pM 5, pH 7.4. This is also in accord with the assignment, since the fraction of dGuo ($N_7$) sites complexed at the higher pH is $\ll$0.1%.

(*C*) *Calf Thymus DNA at pM 5.* Previous attempts to observe slow-passage ODMR signals of calf thymus DNA in the steady state during optical pumping have not been successful. Either there is a vanishing degree of spin alignment in the triplet ensemble or the radiative quantum yields of the sublevels are very similar or both. Using a modified slow-passage method in which the signal is accumulated during the decay of phosphorescence, we have observed the ODMR signals of DNA (Dinse & Maki, 1976) which are assigned to thymine on the basis of the zfs. The ODMR signals of calf thymus DNA observed by slow-passage methods are listed for pM 5 in Table II. The spectrum is quite complex in the frequency range 4–7 GHz, but, since the triplet states involved decay at different rates, we were able to enhance the signals due to the shorter lived triplet states by using rapid repetition rates through the regions where overlapping transitions occur. On the basis of the zfs frequencies and signal polarities, signals at 4.58 and 5.99 GHz are assigned to G ($N_7$) complexes (Table II). Complexing with G at $N_1$ is ruled out on the basis of the zfs parameters. The $\nu_1$ signal (1.37 GHz) assigned to G ($N_7$) is [−] in DNA, whereas this signal is [+] in GMP ($N_7$) and in poly(dG)·poly(dC). The change in polarity may be due to differences in the sublevel populating pattern in DNA relative to the model systems or to changes in the sublevel decay rate constants resulting from stacking interactions with near neighbors. The remaining signals have zfs frequencies and an intensity pattern which are the same as those found in poly(dA)·poly(dT) at pM 6. The frequencies are also close to those found for 3-MeCyd complexed at $NH_2$ (Table II), but this binding site is unlikely at pM 5 based on the monomer equilibrium constant measurements (Simpson, 1964). Also, these signals were not observed in poly(dG)·poly(dC) at pM 5. The $\nu_1$ signals assigned to G ($N_7$) and to T are shown in Figure 5. While the $\nu_1$ signal assigned to G ($N_7$) is symmetrical at the relatively rapid sweep rate in this measurement, indicating that the sublevel lifetimes are considerably shorter than the passage time, it will be noted that the $\nu_1$ signal assigned to T shows rapid-passage effects even at the slower passage rate, indicating that the response time of the more radiative sublevel involved in the transition is longer than the passage time. When the $\nu_1$ signal of T is swept in the opposite direction, the observed response is a mirror image of that seen in Figure 5A, demonstrating that the unsymmetrical appearance of this signal is the result of rapid passage effects rather than an inherently unsymmetrical line shape. We have attempted to measure the phosphorescence transient response of this signal under genuine rapid-passage conditions but find that as the microwave sweep rate through the signal is increased, the intensity of the response rapidly vanishes. We do not understand this behavior, since we generally find that inhomogeneously broadened ODMR signals increase in intensity under rapid-passage conditions.[2] A rough estimate of the transient response lifetime of the transition can be made,

[2] The rapid passage signal intensity of the $T_i \rightarrow T_j$ transition is proportional to the difference in radiative rate constants, $(k_i^{(r)} - k_j^{(r)})$, while the slow passage intensity is proportional to the difference in radiative quantum yields $(Q_i - Q_j)$. $Q_{i,j} = k^{(r)}_{i,j}/k_{i,j}$, where $k_{i,j}$ is the overall decay constant. Thus it is possible that for the $\nu_1$ transition, the $Q$'s are substantially different while the $k^{(r)}$'s are nearly the same.

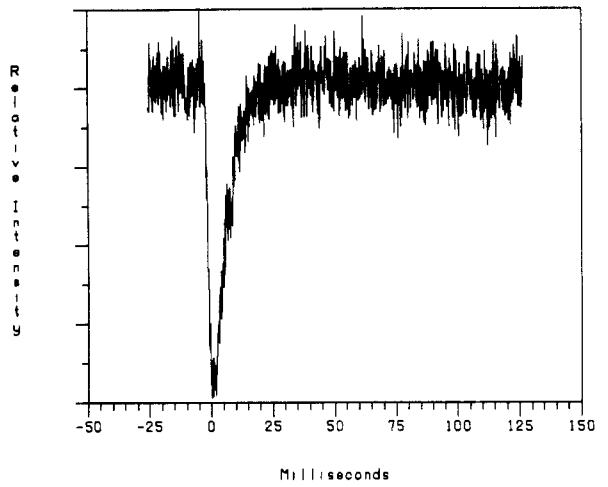


FIGURE 6: Microwave-induced phosphorescence transient resulting from rapid passage through the 1.37-GHz $\nu_1$ signal of calf thymus DNA at pM 5. The rapid passage occurs at $t = 0$, and the signal results from 31 000 accumulations. $T = 1.2$ K.

nonetheless, from the signal observed in Figure 5A. We estimate that the transition has a response time of 100 ms (±50%). When comparisons with the lifetimes observed for this transition in poly(dA)·poly(dT) (Table III) are made, we see that the response is much longer than that observed at pM 5 but is consistent with the lifetimes observed at pM 6 and pM ∞.

We did succeed, however, in measuring the transient phosphorescence response of the signal in Figure 5B which we have assigned as $\nu_1$ of a G ($N_7$) complex. The response, which is shown in Figure 6, decays with a $1/e$ lifetime of 6 ms, confirming that the signal results from a short-lived triplet state. This short lifetime is consistent with the symmetrical appearance of the slow-passage signal (Figure 5B) and is in reasonable agreement with that found for the $\nu_1$ signal of poly(dG)·poly(dC) at pM 5 which supports its assignment to the G ($N_7$) complex.

The ODMR signals of DNA complexed with $CH_3Hg^{II}$ at pM 5 which we assign to T have the polarity pattern [+][−][+], and the triplet state has relatively long-lived sublevels. This behavior is similar to that found in poly(dA)·poly(dT) when complexed at pM 6. Since no slow-passage signals from thymine can be observed in uncomplexed DNA, the thymine signals observed at pM 5 must be induced by $CH_3Hg^{II}$ binding in their entirety. We suggest that there are complexes formed in DNA at pM 5 and in poly(dA)·poly(dT) at pM 6 which are similar and that the Hg atom is sufficiently distant from thymine that heavy-atom effects are minimal, or essentially not present. Since $N_3$ of dThd is the strongest base binding site for $CH_3Hg^{II}$ near neutral pH and since the ODMR demonstrates that these complexes are not present in the polynucleotides, it is unlikely that the $CH_3Hg^{II}$ is bound by a simple monomer interaction. It is possible that the duplex structure provides complex binding sites of $CH_3Hg^{II}$ which have great stability. Although these stable binding sites do not involve the close approach of the Hg atom to dThd, other heterocyclic bases with higher triplet energies than that of T could interact with the Hg atom, and the triplet yield could be enhanced by a heavy-atom effect. The pattern of energy transfer to T in the polymer might thus be altered and provide a mechanism for (a) the altered character of the T signals in poly(dA)·poly(dT) upon complexing with $CH_3Hg^{II}$ at pM 6 and (b) the appearance of similar T signals in DNA at pM 5. Other possibilities exist, including the presence of a vestigial heavy-atom effect as a consequence of the binding of $CH_3Hg^{II}$ at a site which is remote from dThd; we cannot be more specific at this time. It is significant that we do not observe complexes of $CH_3Hg^{II}$ with $N_3$ of T at pM 5 in calf thymus DNA. The disruption of local structure necessary for the formation of thymine $N_3$ complexes with $CH_3Hg^{II}$ may be more difficult to achieve in the calf thymus DNA duplex, or it may not occur at all without the cooperative denaturation observed at lower pM (Gruenwedel & Davidson, 1967).

We observe short-lived heavy atom perturbed T signals in calf thymus DNA which have the ODMR pattern [+][+][+] at higher $CH_3Hg^{II}$ concentrations (pM in the range 3–4). The signals occur at the same frequencies as those found for TMP ($N_3$), and we believe that these DNA signals result from T complexing at this site. At such a high concentration of $CH_3Hg^{II}$, however, the sample may be in a denatured form.

## Conclusions

We have found that complexing of $CH_3HgOH$ with poly(dA)·poly(dT), with poly(dG)·poly(dC), and with calf thymus DNA occurs at concentrations well below those which have previously been found necessary to cause denaturation of the duplex and massive binding of $CH_3Hg^{II}$ to dThd ($N_3$) and to dGuo ($N_1$). The presence of $CH_3Hg^{II}$–base complexes is detected by the appearance of a heavy-atom effect which induces short-lived components in the phosphorescence decay of the polynucleotide. The heavy atom perturbed bases are identified by ODMR on the basis of their characteristic spectra, which have been measured for model mononucleotide and mononucleoside complexes. At pM 5, $CH_3Hg^{II}$ forms complexes with $N_3$ of dThd in poly(dA)·poly(dT), and it is proposed that the duplex remains intact but that there is local disruption of the base pairing to accommodate the complexing. At pM 5, $CH_3Hg^{II}$ forms complexes with $N_7$ of dGuo in both calf thymus DNA (pH 6.8) and poly(dG)·poly(dC) (pH 6.0), but no dThd ($N_3$) complexes are detected in DNA. At pM 6, changes are observed in the thymine ODMR signals of poly(dA)·poly(dT), which are indicative of binding of $CH_3Hg^{II}$ to the polynucleotide but which do not necessarily arise from a heavy-atom effect. These signals are found in calf thymus DNA at pM 5, even though no slow-passage signals are found in uncomplexed DNA. Based on the zfs frequencies, these signals arise from thymine, although the nature of the complexes responsible for these signals is not understood except to the extent that the close approach of Hg to T is not involved. These complexes are quite stable, since the effects are observed in poly(dA)·poly(dT) at pM 6.

## References

Anderson, R. R. (1979) Ph.D. Thesis, University of California, Davis, CA.

Anderson, R. R., & Maki, A. H. (1977) *Photochem. Photobiol. 25*, 585–589.

Chrisman, R. W., Mansy, S., Peresie, H. J., Ranade, A., Berg, T. A., & Tobias, R. S. (1977) *Bioinorg. Chem. 7*, 245–266.

Clegg, M. S., & Gruenwedel, D. W. (1979) *Z. Naturforsch. C: Biosci. 34C*, 259–265.

Co, T., & Maki, A. H. (1978) *Biochemistry 17*, 182–186.

Dinse, K. P., & Maki, A. H. (1976) *Chem. Phys. Lett. 38*, 125–129.

Eisinger, R. J., & Shulman, R. G. (1968) *Science (Washington, D.C.) 161*, 1311–1319.

El-Sayed, M. A. (1972) *MTP Int. Rev. Sci.: Phys. Chem. Ser. One 3*, 119–153.

Giachino, G. C., & Kearns, D. R. (1970a) *J. Chem. Phys. 52*, 2964–2974.

Giachino, G. G., & Kearns, D. R. (1970b) *J. Chem. Phys. 53*, 3886–3891.

Gruenwedel, D. W. (1972) *Eur. J. Biochem. 25*, 544-549.
Gruenwedel, D. W., & Davidson, N. (1966) *J. Mol. Biol. 21*, 129-144.
Gruenwedel, D. W., & Davidson, N. (1967) *Biopolymers 5*, 847-861.
Gruenwedel, D. W., & Lu, D. S. (1970) *Biochem. Biophys. Res. Commun. 40*, 542-548.
Hoover, R. J., Luk, K. F. S., & Maki, A. H. (1974) *J. Mol. Biol. 89*, 363-378.
Kasha, M. (1952) *J. Chem. Phys. 20*, 71-74.
Kuan, T. S., Tinti, D. S., & El-Sayed, M. A. (1970) *Chem. Phys. Lett. 4*, 507-510.
Kwiram, A. L. (1972) *MTP Int. Rev. Sci.: Phys. Chem. Ser. One 4*, 271-316.
Maki, A. H., & Co, T. (1976) *Biochemistry 15*, 1229-1235.
Millar, D. B. (1968) *Biochim. Biophys. Acta 166*, 628-635.
Simpson, R. B. (1964) *J. Am. Chem. Soc. 86*, 2059-2065.
Walter, A., & Luck, G. (1977) *Nucleic Acids Res. 4*, 539-550.
Waugh, T. D., Walton, H. F., & Laswick, J. A. (1955) *J. Phys. Chem. 59*, 395-399.
Winscom, C. J., & Maki, A. H. (1971) *Chem. Phys. Lett. 12*, 264-268.
Yamane, T., & Davidson, N. (1961) *J. Am. Chem. Soc. 83*, 2599-2607.

# Transient Permeabilization Induced Osmotically in Membrane Vesicles from *Torpedo* Electroplax: A Mild Procedure for Trapping Small Molecules†

Larry K. West* and Leaf Huang

ABSTRACT: During hypoosmotic stress, membrane vesicles enriched in acetylcholine receptors become more permeable to external tracer molecules. When vesicles are immersed in 3 volumes of water containing $^{22}Na^+$, 50-70% of $^{22}Na^+$ equilibration is attained within 90 s. On the other hand, the uptake of $^{22}Na^+$ is greatly diminished only 6-10 s after an osmotic shock, and vesicle resealing is completed within 15 s. Furthermore, 90 s after osmotic shock, efflux rates are comparable to those of native vesicles, which also indicates that the vesicles have resealed. During osmotic shock, the entry of molecules into the vesicles increases with the strength of the osmotic shock and also depends on the size of the permeant. With a given strength of osmotic shock, the large molecule [$^3$H]inulin ($M_r$ 5000) is taken up less than the smaller molecules $^{22}Na^+$ and [$^3$H]sucrose. In addition, $\alpha$-bungarotoxin binding latency of the vesicles is not affected by osmotic shock, indicating that the sideness of the vesicles remains unchanged. The acetylcholine receptors in the vesicles remain functional after osmotic shock. For example, 90 s after $^{22}Na^+$ and [$^3$H]sucrose are loaded into vesicles by osmotic shock, only $^{22}Na^+$ is released by dilution in a buffer containing carbamoylcholine (carbamylcholine). Also, the influx of $^{22}Na^+$ into previously shocked vesicles can be specifically stimulated by carbamoylcholine. Such stimulations in the shocked vesicles can be blocked by *d*-tubocurarine or $\alpha$-bungarotoxin, and they can be desensitized by preincubation with carbamoylcholine. These results suggest the possibility of using osmotic shock to load molecular probes into these membrane vesicles, which could provide a powerful tool for studying inner surfaces of the intact vesicles.

Knowledge of neuromuscular transmission has been extended by studies on electric eels and rays, from which membrane vesicles (microsacs) enriched in nicotinic acetylcholine receptors can be obtained in relatively large quantities (Heidmann & Changeux, 1978). In general, cholinergic stimulation results in increased postsynaptic membrane permeability to alkali cations, and the in vitro counterpart of cholinergic excitability is a rapid release of tracer cations from preloaded membrane vesicles when they are exposed to agonists. The cholinergic responses of acetylcholine receptor containing vesicles isolated from eels and rays have been documented in a variety of studies (Heidmann & Changeux, 1978; Neubig et al., 1979; Eldefrawi et al., 1978; Bernhardt & Neumann, 1978; Hess et al., 1978; Lindstrom & Patrick, 1974; Miller et al., 1978; Moore et al., 1979), but, until recently (Hartig & Raftery, 1979), no isolated membrane preparations were available for studying the external and internal surfaces of the membranes independently. The preparation of Hartig & Raftery (1979) consists of right side out vesicles, an excellent material for studying the external vesicle surface. However, a method is needed to gain experimental access to the inner vesicle surface. We report here (1) a potential method to load molecular probes into acetylcholine receptor membrane vesicles by osmotic shock, (2) the early changes in membrane permeability that accompany exposure of the vesicles to osmotic stress, and (3) the effect of osmotic shock on the functional integrity of the acetylcholine receptor and on its orientation in the membrane.[1]

## Materials and Methods

*Preparation of Acetylcholine Receptor Enriched Membranes.* Acetylcholine receptor enriched membranes were prepared isotonically from frozen electric organs of *Torpedo californica* (Pacific Biomarine, Venice, CA) essentially as described by Miller et al. (1978), with two exceptions: (1) 100 $\mu$M phenylmethanesulfonyl fluoride was included in

† From the Department of Biochemistry, University of Tennessee, Knoxville, Tennessee 37916. *Received February 13, 1980.* This research was supported by National Institutes of Health Grants GM23473 and CA24553 and by a Muscular Dystrophy Association of America Postdoctoral Fellowship to L.K.W.

[1] A preliminary account of this study has been reported previously (West & Huang, 1979). After this paper was submitted for publication, we learned that similar observations have been made by others (P. R. Hartig, H.-P. H. Moore, and M. A. Raftery, personal communication).

0006-2960/80/0419-4418$01.00/0 